

Transient Times of Fission in $^{40}\text{Ar} + ^{232}\text{Th}$ Peripheral Collisions

E.-M. Eckert, A. Kühmichel, and J. Pochodzalla
Universität Frankfurt, D-6000 Frankfurt, West Germany

K. D. Hildenbrand, U. Lynen, W. F. J. Müller, H. J. Rabe, H. Sann, H. Stelzer, W. Trautmann,
 R. Trockel, and R. Wada^(a)
Gesellschaft für Schwerionenforschung Darmstadt, D-6100 Darmstadt, West Germany

C. Cerruti, P. Lhénoret, R. Lucas, C. Mazur, C. Ngô, M. Ribrag, and E. Tomasi
Centre d'Etudes Nucleaires de Saclay, F-91191 Gif-sur-Yvette, France

A. Demeyer and D. Guinet
Université Claude Bernard, F-69622 Villeurbanne, France
 (Received 16 January 1990)

Peripheral $^{40}\text{Ar} + ^{232}\text{Th}$ collisions at a bombarding energy $E/A = 30$ MeV were studied by measuring coincidences of fission fragments with projectile fragments detected near the grazing angle. It is found that the sequential fission of the highly excited target residue nuclei is severely hindered if their excitation energies, determined from the measured recoil momenta, exceed a value of about 50–75 MeV. A transient time of fission of the order of 10^{-20} s is deduced.

PACS numbers: 25.70.Np, 25.85.Ge

Fission is generally believed to be a slow process since it involves a major rearrangement of nuclear matter. Experimental evidence for a time delay of fission has been reported by several groups in recent years (Refs. 1–4, and references given therein). It is mainly based on the multiplicities of evaporated light particles determined separately for the emission from the composite system and from the fully accelerated fragments.^{1–3} Conceptually, the time elapsing before scission may be divided into (i) the transient time τ_t needed to build up the probability flux across the barrier and to irreversibly enter the fission channel,⁵ and (ii) the time τ_{ss} to subsequently descend from saddle to scission. The particle-multiplicity experiments are sensitive to the sum of both times, and attempts to deduce the individual contributions have to rely on model calculations.^{1,3}

The magnitude of the transient time is of particular importance in the case of highly excited nuclei. If the evaporation times become shorter than the transient time, fission cannot compete with nucleon emission as expected on the basis of phase-space considerations alone and will be hindered. Similar transient effects may also exist in other macroscopic decay modes such as the emission of intermediate-mass fragments or multifragmentation.⁶ Recently, Thoennessen *et al.* reported an enhancement of the prefission giant-dipole-resonance decay of thorium nuclei, excited up to 80 MeV, which was explained by a fission hindrance in the early decay steps.⁴ In the present work, the existence of finite transient times in fission is inferred from the measured fission probabilities of target residues of up to $\cong 200$ -MeV excitation which were produced in peripheral $^{40}\text{Ar} + ^{232}\text{Th}$ collisions. The initial excitation energies and spins of

these nuclei, necessary for the comparison to statistical-model calculations, were deduced from the measured linear momentum transfer.

Metallic self-supporting ^{232}Th targets with areal density 1.0 mg/cm² were bombarded with a ^{40}Ar beam of energy $E/A = 30$ MeV provided by the SARA facility in Grenoble. Projectilelike fragments (PLF's) were detected and identified according to their atomic number Z_{PLF} with an ionization chamber covering the range $6.3^\circ \leq \Theta_{\text{lab}} \leq 13.7^\circ$ around the grazing angle of $\Theta_{\text{lab}} \cong 9^\circ$. Fission fragments were detected with an array of twelve parallel-plate avalanche counters (PPAC's) mounted symmetrically around the target and subtending a solid angle of $\Delta\Omega = 2.3\pi$ sr in the range $22^\circ \leq \Theta_{\text{lab}} \leq 158^\circ$. The PPAC array was backed by an array of ten plastic detectors⁷ of 1-cm thickness covering a solid angle $\Delta\Omega = 1.8\pi$ sr at $23^\circ \leq \Theta_{\text{lab}} \leq 157^\circ$.

Projectilelike fragments with $Z_{\text{PLF}} \geq 12$ were stopped in the ionization chamber. Their energy spectra are characteristic of peripheral collisions and exhibit nearly symmetric distributions centered at specific energies E/A slightly smaller than that of the beam.⁸ The coincidence data were sorted according to Z_{PLF} , and the derived results are given in Table I as averages for the $12 \leq Z_{\text{PLF}} \leq 17$ channels. The linear momenta p_{\parallel} transferred to the targetlike fragments (TLF's) parallel to the beam direction were determined from the fission-fragment folding angles measured with the PPAC array.⁹ The momentum transfer increases monotonically with decreasing Z_{PLF} as observed for other reactions.¹⁰ At the same time an increasing number of fast, light particles is emitted as evident from the momentum deficit Δp_{\parallel} , defined as the difference between the beam momen-

TABLE I. Measured and derived results.

Z_{PLF}	$\langle p_{\parallel} \rangle^a$ (GeV/c)	$\langle \Delta p_{\parallel} \rangle$ (GeV/c)	$\langle \Delta Z \rangle$	$\langle Z_{\text{res}} \rangle$	$\langle E_x \rangle^a$ (MeV)	$\langle I \rangle^a$ (\hbar)	P_f^a
17	0.39	0.6 ± 0.1	2.5 ± 0.6	88.5 ± 0.6	49	14	0.52
16	0.59	1.0 ± 0.1	3.5 ± 0.7	88.5 ± 0.7	74	20	0.56
15	0.92	1.4 ± 0.2	4.3 ± 0.8	88.7 ± 0.8	116	31	0.72
14	1.10	1.7 ± 0.2	5.1 ± 1.0	88.9 ± 1.0	139	36	0.62
13	1.45	2.3 ± 0.3	6.4 ± 1.2	88.6 ± 1.2	183	47	0.55
12	1.74	2.5 ± 0.4	7.3 ± 1.4	88.7 ± 1.4	219	55	0.44

^aThe experimental error is about $\pm 10\%$.

tum and the sum of the PLF and TLF parallel momenta.

The average number of charges carried away by light particles $\langle \Delta Z \rangle$ was determined from the charged-particle multiplicity measured with the plastic array at $\Theta_{\text{lab}} > 23^\circ$ and by referring to the literature¹¹⁻¹³ for the remaining range of forward angles. The data from the plastic array were solid-angle corrected and an average charge of 1.5 per charged particle¹¹ was assumed. The multiplicities at very forward angles depend on the target mass and the bombarding energy sufficiently weakly¹³ so that the data¹² for $^{40}\text{Ar} + \text{Ag}$ at $E/A = 35$ MeV could serve as rather good estimates. The average residual charge $\langle Z_{\text{res}} \rangle = 90 + 18 - Z_{\text{PLF}} - \langle \Delta Z \rangle$ is between 88 and 89 for all six Z_{PLF} channels. It is known that neutron evaporation strongly dominates in these peripheral reactions and that the average multiplicities of light, charged particles evaporated from the TLF's are negligible in comparison.¹⁴ Thus the observed charged particles are either of preequilibrium nature or emitted by the PLF's, and $\langle Z_{\text{res}} \rangle$ is essentially equal to the average atomic number $\langle Z_{\text{TLF}} \rangle$ of the initial TLF's (after preequilibrium emission).

The mean excitation energies $\langle E_x \rangle$ and spins $\langle I \rangle$ transferred to these nuclei were determined from their linear momenta $\langle p_{\parallel} \rangle$ by using the kinematics of a massive transfer process. The linear correlations of E_x and I with p_{\parallel} that are expected in that case have been observed in peripheral reactions in the intermediate energy regime.^{14,15} The obtained mean values $\langle E_x \rangle = v_0 \langle p_{\parallel} \rangle / 2$ (v_0 is the projectile velocity) reach up to more than 200 MeV (Table I). These excitation energies correspond to the time right after preequilibrium emission when the recoil velocity, on the average, remains unaltered by the subsequent evaporation cascades. They agree quite well with the excitation energies derived from neutron multiplicity measurements which are sensitive to the evaporative component.¹⁴ The radii R needed to calculate the transferred angular momenta $\langle I \rangle = R \langle p_{\parallel} \rangle$ were determined from an overlap geometry which was calibrated by applying the same procedure to the experimental data of Namboodiri *et al.*¹⁵ The variation from $R = 6.9$ fm for $Z_{\text{PLF}} = 17$ to $R = 6.2$ fm for $Z_{\text{PLF}} = 12$ reflects the decrease in impact parameter with increasing energy and momentum transfer. The maximum spin transfer $\langle I \rangle$

$= 55\hbar$ for $Z_{\text{PLF}} = 12$ is still considerably less than the value of about $80\hbar$ at which the fission barrier is expected to vanish.¹⁶ We also note in this context that the ground-state deformation¹⁷ $\beta = 0.26$ of the target is smaller than the calculated¹⁸ saddle-point deformations $\beta \cong 1.0$ of the excited TLF's. The system thus starts from inside the saddle-point configuration which represents a methodical advantage compared to heavy-ion fusion reactions.

The fission probabilities P_f were determined from the measured ratios of inclusive and fission-coincident PLF's. The efficiency of the PPAC array to record both fission fragments, $\epsilon = 0.37 \pm 0.04$, was obtained from a Monte Carlo model which took the properties of the detectors and the observed angular distributions of the fission fragments into account. The 10% error margin represents the experimental uncertainty of P_f . The resulting fission probabilities first increase with decreasing Z_{PLF} up to $P_f \cong 0.7$ and then decrease to values $P_f < 0.5$ (Table I).

The fission probabilities expected within the statistical model for TLF's excited to the initial energies and spins associated with the six Z_{PLF} channels were calculated with the code HIVAP (Ref. 19) for a variety of nuclei with atomic numbers Z around $\langle Z_{\text{res}} \rangle$. The fission barriers from the prescription of Sierk¹⁶ and the fissility-dependent a_f/a_n parameters suggested by Töke and Swiatecki^{19,20} were used ($1.05 \leq a_f/a_n \leq 1.09$). The resulting probabilities depend strongly on Z_{TLF} for the lower excitations ($Z_{\text{PLF}} = 16, 17$) and there, within the errors, agree rather well with the measured values (Fig. 1, top). This is not the case for the higher excitations for which $P_f \cong 1$ is predicted but not observed.

The choice of a_f/a_n has a strong influence on the calculated fission probabilities. In Fig. 1, bottom, the results of a second set of calculations with $a_f/a_n = 1.0$ and fission barriers equal to 85% of the Sierk barriers are shown. The effects of the two modifications compensate each other in such a way that nearly identical results are obtained for $Z_{\text{PLF}} = 17$. At the higher excitations the fission probabilities do not increase quite as fast as in the previous case and the deviation from the experiment becomes significant only at $E_x > 120$ MeV ($Z_{\text{PLF}} < 15$). This coincides with the range of excitations where the measured decrease of P_f with increasing energy and spin

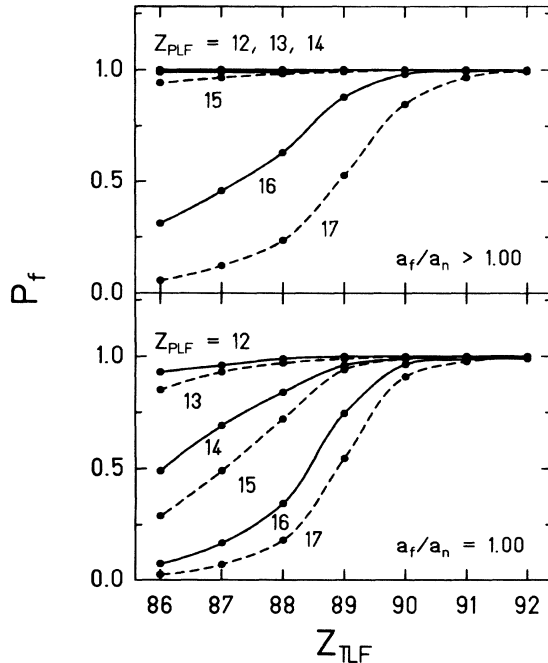


FIG. 1. Calculated fission probabilities P_f for the excitation energies and spins reached in the $12 \leq Z_{PLF} \leq 17$ channels (see Table I) as a function of Z_{TLF} [$A_{TLF} \cong 230 + 2.4(Z_{TLF} - 89)$] and for two-parameter sets (see text). The lines are meant to guide the eye.

establishes a discrepancy with any statistical expectation, independent of the choice of parameters, and even if a broad element distribution is assumed for the initial TLF's (Fig. 1). In the calculations, a higher initial excitation always leads to a higher fission probability since the extra deexcitation steps add to it while the evaporation of a few more neutrons does not effectively alter the fissility of the decaying TLF (the proton-to-neutron branching ratios are on the percent level in accordance with the experimental observation¹⁴).

There is a solid physical basis for the surface effects that lead to $a_f/a_n > 1$ and thus for the more rapid rise of the statistically expected fission probability with excitation energy.¹⁹⁻²¹ Comparing with the results obtained with the first parameter set we may therefore conclude that the fission hindrance sets in at excitation energies clearly below 120 MeV (Fig. 1, top). With the argument that $\langle Z_{TLF} \rangle$ is most likely a smooth function of Z_{PLF} , this upper limit is lowered to 75 MeV. In fact, if the statistical prediction is assumed to be still valid at $E_x \cong 50$ MeV, then the measured $P_f = 0.52$ ($Z_{PLF} = 17$) requires $\langle Z_{TLF} \rangle \cong 89$ where the measured $P_f = 0.56$ at $E_x \cong 75$ MeV ($Z_{PLF} = 16$) is highly overpredicted. This result agrees with the observation of Thoennessen *et al.*⁴

In order to demonstrate the effect of a finite transient time and to qualitatively understand the measured fission probabilities at the higher excitations, we have performed further statistical calculations within the follow-

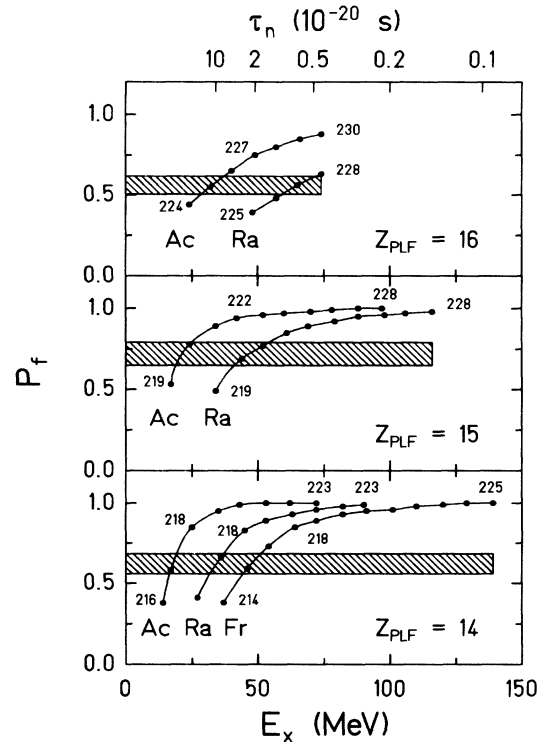


FIG. 2. Calculated fission probabilities P_f along the most probable neutron evaporation paths (see text) for the examples of $Z_{PLF} = 14, 15,$ and 16 and for cascades starting from excited ^{230}Ac , ^{228}Ra , or ^{225}Fr nuclei (the $a_f/a_n > 1$ parameter set as for Fig. 1, top, was used). Some of the mass numbers reached along the neutron cascades are indicated. The hatched areas mark the measured fission probabilities.

ing scheme. First, the most probable evaporation sequences in the absence of fission were determined by using the HIVAP code with the fission probability artificially set to zero. Then the fission channel was turned on again, and fission probabilities were calculated for each step n along these sequences, i.e., for the nuclide, energy, and spin reached after $n-1$ evaporation steps. In Fig. 2 the results are shown for the channels $Z_{PLF} = 14, 15,$ and 16 and for pure neutron cascades starting from excited ^{230}Ac , ^{228}Ra , or ^{225}Fr nuclei. The so-determined fission probabilities decrease along the evaporation paths and at some point cross the range of the experimental values. The agreement with the statistical model is thus recovered if fission is assumed to be hindered until the neutron cascades have deexcited the initial TLF's to that point or, more generally, to energies in that range, depending on the elemental composition of the TLF's. The crossover energies are of the order of 50 MeV or less (Fig. 2) which, within the limitations of this schematic picture, is consistent with the apparent onset of the fission hindrance.

Typical values of the calculated neutron evaporation times τ_n encountered along the evaporation paths are shown on the top abscissa scale of Fig. 2 ($a_n = A/8.0$ as

used). Their rapid increase with decreasing excitation energy has the effect that the integrated emission time of a cascade is dominated by the time needed for the last step of the sequence.^{2,3} The magnitude of the transient time is thus approximately given by $\tau_t \cong \tau_n(E_x)$ where E_x corresponds to the onset of the fission hindrance. For E_x between 50 and 75 MeV, τ_t is in the range of $(0.5-2) \times 10^{-20}$ s. These values are larger than present estimates²² for saddle-to-scission times of several 10^{-21} s, which implies that in these reactions the transient time is the dominant contribution to the total time elapsing before scission. As stated before, this last conclusion relies on the physical arguments that are at the basis of the fissility-dependent level-density parameters¹⁹⁻²¹ whereas the mere existence of a finite transient time of more than 10^{-21} s, corresponding to $E_x \cong 120$ MeV, follows from the present work independent of these considerations.

We are highly indebted to the staff of the SARA facility in Grenoble for providing an excellent ^{40}Ar beam and W. Quick for essential contributions to the experimental setup. We would like to thank W. Reisdorf for assistance in using the code HIVAP and for helpful discussions.

^(a)Present address: Texas A&M University, College Station, TX 77843.

- ¹A. Gavron *et al.*, Phys. Rev. C **35**, 579 (1987).
- ²D. Hilscher *et al.*, Phys. Rev. Lett. **62**, 1099 (1989).
- ³D. J. Hinde *et al.*, Phys. Rev. C **39**, 2268 (1989).
- ⁴M. Thoennessen *et al.*, Phys. Rev. Lett. **59**, 2860 (1987).
- ⁵P. Grangé, Li Jun-Quing, and H. A. Weidenmüller, Phys. Rev. C **27**, 2063 (1983).
- ⁶J. Pochodzalla *et al.*, Phys. Rev. C **40**, 2918 (1989).
- ⁷H. J. Rabe *et al.*, Phys. Lett. B **196**, 439 (1987).
- ⁸V. Borrel *et al.*, Z. Phys. A **324**, 205 (1986).
- ⁹E.-M. Eckert, thesis, Universität Frankfurt, 1988 (unpublished); E.-M. Eckert *et al.* (to be published).
- ¹⁰J. L. Laville *et al.*, Phys. Lett. **138B**, 35 (1984).
- ¹¹D. Jacquet *et al.*, Phys. Rev. C **32**, 1594 (1985).
- ¹²G. Bizard *et al.*, Phys. Lett. B **172**, 301 (1986).
- ¹³J. C. Steckmeyer *et al.*, Nucl. Phys. **A500**, 372 (1989).
- ¹⁴M. Morjean *et al.*, Phys. Lett. B **203**, 215 (1988); J. Galin *et al.*, in *Proceedings of the Symposium on Nuclear Dynamics and Nuclear Disassembly*, edited by J. B. Natowitz (World Scientific, Singapore, 1989), p. 320; D. X. Jiang *et al.*, Nucl. Phys. **A503**, 560 (1989).
- ¹⁵M. N. Namboodiri *et al.*, Phys. Rev. C **35**, 149 (1987).
- ¹⁶A. J. Sierk, Phys. Rev. C **33**, 2039 (1986).
- ¹⁷S. Raman *et al.*, At. Data Nucl. Data Tables **36**, 1 (1987).
- ¹⁸H. Feldmeier (private communication).
- ¹⁹W. Reisdorf *et al.*, Nucl. Phys. **A444**, 154 (1985); (private communication).
- ²⁰J. Töke and W. J. Swiatecki, Nucl. Phys. **A372**, 141 (1981).
- ²¹S. E. Vigdor and H. J. Karwowski, Phys. Rev. C **26**, 1068 (1982).
- ²²J. R. Nix, Nucl. Phys. **A502**, 609c (1989).